Accepted Manuscript

International Journal of Nanoscience

Article Title:	Fabrication and Properties of Molybdenum Disulfide Films for Electro-Optical Applications
Author(s):	S. Ozcelik, N. Akcay, M. Tivanov
DOI:	10.1142/S0219581X19400374
Received:	22 December 2018
Accepted:	14 January 2019
To be cited as:	S. Ozcelik, N. Akcay, M. Tivanov, Fabrication and Properties of Molybdenum Disulfide Films for Electro-Optical Applications, *International Journal of Nanoscience*, doi: 10.1142/S0219581X19400374
Link to final version:	https://doi.org/10.1142/S0219581X19400374

World Scientific
www.worldscientific.com

International Journal of Nanoscience
Vol. 1, No. 1 (2019) 1–4

FABRICATION AND PROPERTIES OF MOLYBDENUM DISULFIDE FILMS FOR ELECTRO-OPTICAL APPLICATIONS

S. Ozcelik
Gazi University, Photonics Application & Research Center
Gazi University, Physics Department of Science Faculty
06500 Ankara, Turkey
sozcelik@gazi.edu.tr

N. Akcay
Faculty of Engineering, Department of Mechanical Engineering, Baskent University
06790 Ankara, Turkey
Gazi University, Photonics Application & Research Center
06500 Ankara, Turkey
neslihanakcay@baskent.edu.tr

M. Tivanov
Faculty of Physics, Belarusian State University,
Nezavisimosti av. 4, 220050 Minsk, Belarus
tivanov@bsu.by

Received 22 December 2018; accepted 14 January 2019

MoS_2 films on sapphire and SiO_2/Si substrates were fabricated by sulfurization of sputtered Mo precursor films at 900 °C in a two-zone furnace. Structural, morphological, optical and electrical properties of the films were determined. The films of MoS_2 were successfully grown on the substrates with polycrystalline structures and proposed to be used in electro-optical devices.

Keywords: MoS_2 films, molybdenum disulfide, transition metal dichalcogenides, CVD.

1. Introduction

Transition metal dichalcogenides (TMDCs) such as MoS_2, $MoSe_2$, WS_2 and WSe_2 have attracted great interest in recent years because of their excellent electrical, mechanical and optical properties and potential applications in future nanoscale electronic and optoelectronic devices.[1,2] Among these materials, single and multilayer thin films of MoS_2 have the properties different from their three-dimensional bulk counterparts.[3,4] For instance, its band gap exhibits a transition from 1.3 eV for bulk MoS_2 (indirect) to 1.8 eV for single molecular layers (direct) depending on the thickness and this makes it unique for optoelectronic applications.[5] Therefore, this material has been investigated extensively for a wide range of applications such as field effect transistors (FETs),[6] photodetectors,[7] phototransistors,[8] field emitters,[9] solar cells,[10] light emitting diodes[11], and gas sensors.[12]

There have been many various approaches such as exfoliation,[13] hydrothermal synthesis,[14] physical vapor deposition (PVD)[15], and chemical vapor deposition (CVD)[16] for synthesis of MoS_2 thin films. CVD is one of the most promising methods in terms of the possibility of large area and scale-up production of MoS_2 devices in future.

In this study, MoS_2 thin films were fabricated by using the two-step approach: (i) deposition of the Mo precursor films on sapphire and SiO_2/Si substrates by DC magnetron sputtering method, (ii) sulfurization of

Mo films in Ar atmosphere at high temperature in a two-zone CVD furnace with solid phase precursor**.** Structural, morphological, optical and electrical properties of the MoS_2 films were investigated.

2. Experimental

The deposition of Mo films was performed in a magnetron sputtering system equipped with 1 DC and 2 RF two-inch targets confocally (Nanovak, NVTS500). Mo films of about 40 nm thicknesses were deposited on sapphire and SiO_2/Si substrates at room temperature, 5 mTorr pressure of Ar and 60 W power using a 99.95% pure Mo target (2 inch diam. × 0.250 inch thick) by DC magnetron sputtering technique.

After deposition of the Mo precursor films, the sulfurization system was evacuated to ~10^{-3} mbar and purged with Ar gas to remove oxygen and other gases. The sulfurization was carried out at the pressure of 3.4 mbar in a two-zone diffusion furnace by heating of 0.5 g sulfur powder to 250 °C in the first zone and the precursor film to 900 °C in the second zone of the furnace, Fig. 1.

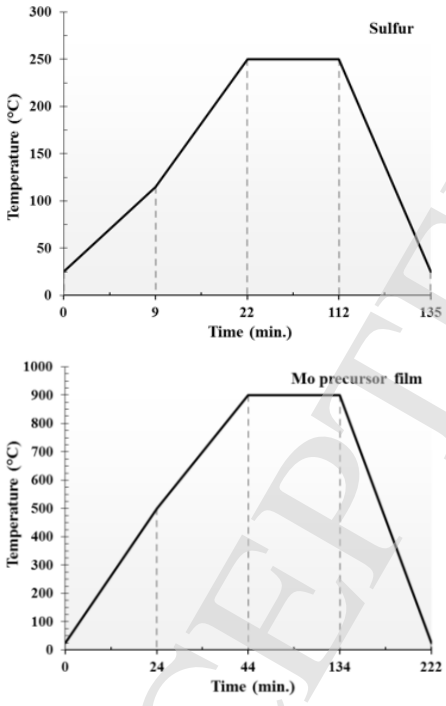

Fig. 1. Temperature profiles in the two-zone furnace during sulfurization process.

Mo films were kept at 900 °C for 1.5 h. The heating rates of S and Mo precursor film zones were ~10 °C/min and ~20 °C/min, respectively. After the sulfurization, both zones of the furnace were cooled down to the room temperature with the rate of 10 °C/min. The thickness of Mo films measured by a profilometer and scanning electron microscopy (SEM) was almost doubled after the sulfurization and raised up to 103 – 125 nm.

X-ray diffraction (XRD) patterns of MoS_2 films were obtained by a APD 2000 PRO X-ray diffractometer in the 2θ range of 20 – 90 deg using CuKα radiation (λ = 1.54052 Å). Raman spectroscopy analysis of the films was carried out at room temperature by using a confocal Raman spectrometer Nanofinder HE (LOTIS TII). For excitation of Raman radiation, a continuous wave solid-state laser with the wavelength of 532 nm was used. SEM analysis was performed in a Hitachi S-4800 (Japan) microscope arranged with an energy dispersive X-ray (EDX) spectrometer. Atomic force microscopy (AFM) measurements were conducted by using a Solver Nano tool (NT-MDT) in the semi-contact mode with a scanning probe of 10 nm tip radius. The optical transmittance and reflectance of MoS_2 films grown on sapphire substrates were measured by using a Perkin Elmer Lambda 2S UV-Vis spectrometer in the wavelength range of 200 – 1100 nm.

3. Results and Discussion

Fig. 2 shows the XRD patterns of MoS_2 films grown on sapphire and SiO_2/Si substrates.

The MoS_2 film grown on sapphire substrate showed three sharp diffraction peaks at 14.39 deg, 32.81 deg and 58.78 deg corresponding to (002), (100) and (110) planes of MoS_2, respectively. The films fabricated on SiO_2/Si substrates showed two diffraction peaks at 32.81 deg and 58.45 deg corresponding to (100) and (110) planes of MoS_2, respectively (JPDS Card 37-1492). In addition, two more peaks were observed at 41.70 deg and 69.16 deg which correspond to the reflection from (113) and (400) planes of sapphire and SiO_2/Si substrates, respectively. Some XRD parameters and calculated lattice constants of MoS_2 films were collected in Table 1.

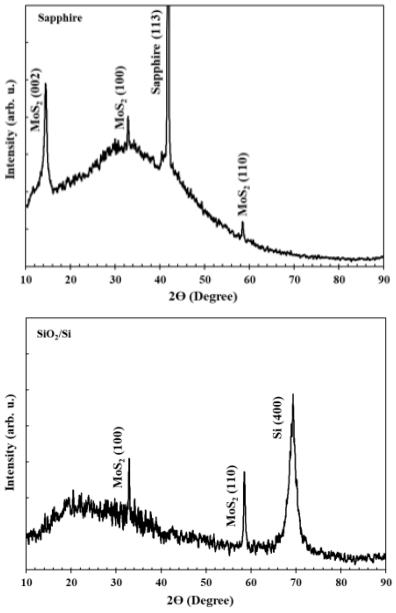

Fig. 2. XRD patterns of MoS_2 films grown on sapphire and SiO_2/Si substrates.

Table 1. Structural parameters calculated from XRD results for MoS_2 films grown on sapphire and SiO_2/Si substrates.

	hkl	2θ (°)	FWHM (°)	a (Å)	c (Å)	Grain size (nm)	Strain (ε) %
Sapphire	002	14.39	0.68	-	12.30	20.42	0.005
	100	32.81	0.37	3.15	-	39.08	-
SiO_2/Si	100	32.81	0.19	3.15	-	74.62	-
	110	58.45	0.38	3.26	-	40.86	-

Raman spectra of the films shown in Fig. 3 demonstrate characteristic E_{2g}, E^1_{2g} and A_{1g} Raman modes of MoS_2 hexagonal phase at around 287 cm^{-1}, 383 cm^{-1} and 409 cm^{-1}, respectively.[17,18] In addition, two peaks located at around 453 cm^{-1} and 466 cm^{-1} were attributed to 2LA(M) and A_{2u} modes.[19]

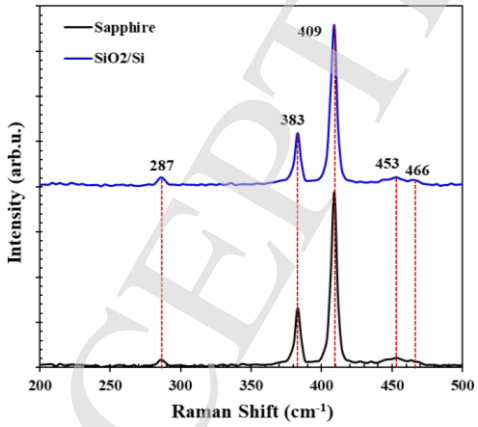

Fig. 3. Raman spectra of MoS_2 films grown on sapphire and SiO_2/Si substrates.

The chemical composition of the MoS_2 films grown on sapphire and SiO_2/Si substrates were determined by EDX technique (Fig. 4). The Mo Lα and S Kα signals were individually determined at ~ 2.4 keV. The atomic and compositional ratios of the elements (Table 2) evidence that non-stoichiometric $MoS_{1.75}$ and $MoS_{1.80}$ films were obtained.

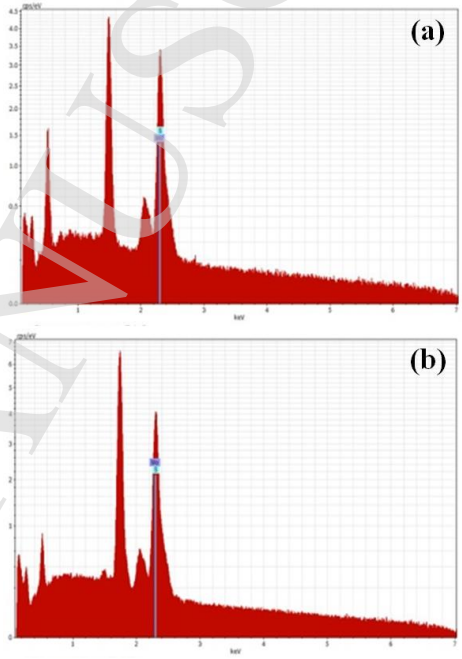

Fig. 4. EDX spectra of MoS_2 films grown on (a) sapphire and (b) SiO_2/Si substrates.

Table 2. Atomic content and compositional ratio in MoS_2 films grown on sapphire and SiO_2/Si substrates.

	Atomic ratio (%)		Compositional ratio (%)
	Mo	S	S/Mo
Sapphire	36.44	63.56	1.75
SiO_2/Si	35.67	64.33	1.80

The surface topography of the films was investigated by AFM analysis. Fig. 5 displays 2D AFM and corresponding 2D grain boundaries images of MoS_2 films. AFM measurements exhibited high RMS roughness values of 27.03 nm and 19.02 nm for the films grown on sapphire and SiO_2/Si substrates, respectively. The film grown on the SiO_2/Si substrate had the smoother surface than the film grown on the sapphire substrate. Also, the film grown on SiO_2/Si substrate had the less amount of grain boundaries with the larger grain size compared to the film grown on sapphire.

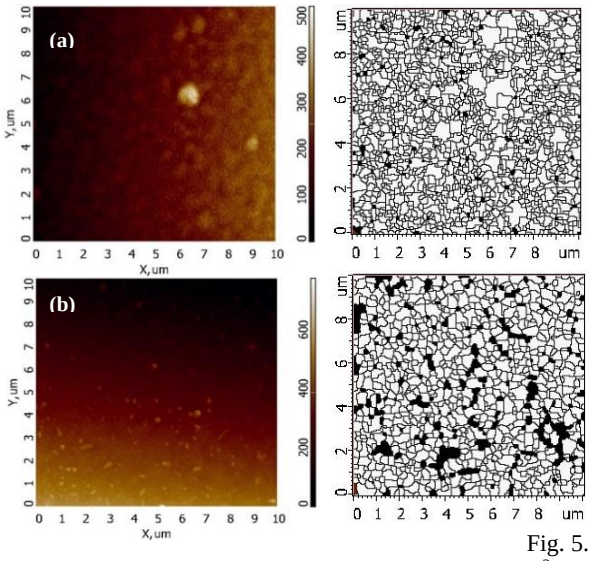

Fig. 5. 2D AFM images and 2D grain boundary images ($10\times10\mu m^2$) of MoS_2 films grown on sapphire (a) and SiO_2/Si (b) substrates.

Top view SEM images are shown in Fig. 6. Both films exhibited uniform morphology with a polycrystalline structure. The crystallites are larger in the film grown on the SiO_2/Si substrate compared to the film grown on the sapphire substrate. These SEM results are consistent with AFM data and grain boundary images, as well as with XRD results. It was seen from Fig. 6b,d that the MoS_2 films possess a densely packed columnar structure without any voids.

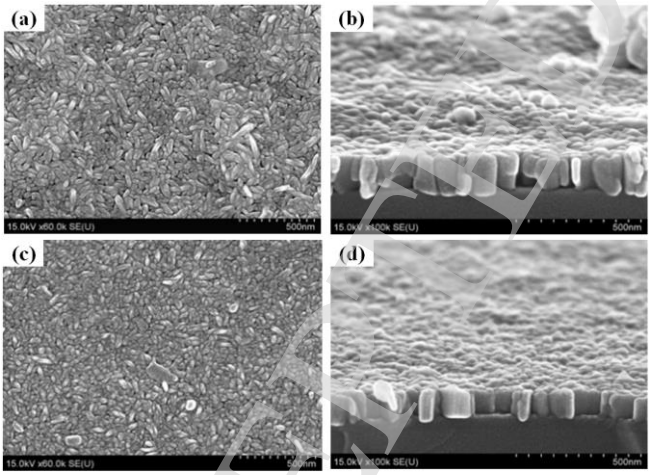

Fig. 6. Surface and cross sectional SEM images of MoS_2 films grown on sapphire (a, b) and SiO_2/Si (c, d) substrates.

Fig. 7 shows the transmittance spectra and the plot of $(\alpha hv)^2$ versus photon energy (hv) of MoS_2 films grown on sapphire substrates. Two minima at 1.84 eV and 2.01 eV corresponding to the transitions at the Brillion zone K point in bulk MoS_2 are observed. The optical absorption coefficient (α) was calculated from the transmission data by using the Beer-Lambert law:

$$\alpha = -\frac{1}{t}\ln(T), \qquad (1)$$

where T is the normalized transmittance and t is the film thickness. The absorption coefficient has the following relationship with the band gap (E_g):

$$(\alpha hv)^n = A(hv - E_g), \qquad (2)$$

where A is a constant and $n = 2$ and $n = 1/2$ for the direct and indirect band gap transitions, respectively.[20] Thus, E_g of the MoS_2 film was found to be 1.58 eV by extrapolating the linear region of the curves to the hv axis.

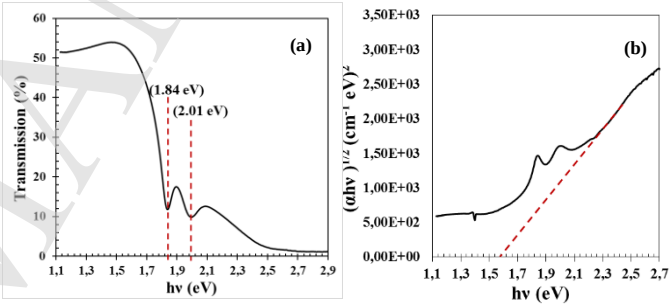

Fig. 7. Transmittance spectra (a) and the plot of $(\alpha hv)^2$ versus photon energy (hv) (b) of the MoS_2 films grown on sapphire substrates.

To determine electrical properties of the MoS_2 films, resistivity and Hall effect measurements were carried out in the constant magnetic field of 0.4 T at 300 K. The measured parameters are listed in Table 3.

Table 3. Electrical properties of MoS_2 films grown on sapphire and SiO_2/Si substrates.

	Resistivity (Ohm·cm)	Carrier Density (1/cm³)	Mobility (cm²/V·s)
SiO_2/Si	$1.90\times10^{+2}$	6.27×10^{13}	150
Sapphire	$7.18\times10^{+2}$	7.03×10^{15}	1.24

The MoS_2 films grown on sapphire and SiO_2/Si substrates are *p*-type semiconductors as was reported by Waldau *et al.*[21] Their resistivity was found to be $7.18\times10^{+2}$ and $1.90\times10^{+2}$ Ohm·cm for sapphire and SiO_2/Si substrates, respectively. Notably, the carrier density in the films grown on sapphire is essentially higher than that in the films on SiO_2/Si substrates.

4. Conclusion

In this study, MoS_2 films on sapphire and SiO_2/Si substrates were fabricated by the Mo precursor films deposition by DC magnetron sputtering followed by sulfurization at 900 °C in a two-zone furnace. It was revealed from XRD and Raman spectroscopy analysis that the polycrystalline MoS_2 films were successfully grown on both substrates. They are non-stoichiometric with composition of $MoS_{1.75}$ and $MoS_{1.80}$, respectively. The RMS roughness of the films on sapphire and SiO_2/Si substrates were found to be 27.03 nm and 19.02 nm, respectively. The MoS_2 films have a uniform surface morphology and the densely packed columnar structure without any voids. E_g of the film material on the sapphire substrate was calculated to be 1.58 eV using UV-Vis transmittance spectra. In addition, both the films grown on SiO_2/Si and sapphire substrates showed *p*-type conductivity with the hole mobility of 150 $cm^2/V{\cdot}s$ and 1.24 $cm^2/V{\cdot}s$, respectively. These results demonstrated that the fabricated films could be used in electro-optical devices as active materials.

Acknowledgments

This work was supported by CSBB (TR) and TUBITAK with 2016K121220 and 118F009 project numbers, and by the Belarusian State Programme for Research «Physical material science, new materials and technologies». The authors of this work are grateful to Affiliate RDC "Belmicrosystems" JSC "INTEGRAL" - "INTEGRAL" Holding Managing Company for SEM studies.

References

1. A. P. Gaur, S. Sahoo, M. Ahmadi, S. P. Dash, M. J. F. Guinel, R. S. Katiyar, *Nano Letters* **14**, 4314 (2014).
2. X. Huang, Y. Gao, T. Yang, W. Ren, H. M. Cheng, T. Lai, *Scientific Reports* **6**, 32236 (2016).
3. Y. Lin, X. Ling, L. Yu, S. Huang, A. L. Hsu, Y. H. Lee, J. Kong, M. S. Dresselhaus, T. Palacios, *Nano Letters* **14**, 5569 (2014).
4. R. Ganatra, Q. Zhang, *ACS Nano* **8**, 4074 (2014).
5. M. Meng, X. Ma, *Nanoscale Res. Lett.* **11**, 513 (2016).
6. B. Radisavljevic, A. Radenovic, J. Brivio, I. V. Giacometti, A. Kis, *Nature Nanotechn.* **6**, 147 (2011).
7. Y. Zhang, Y. Yu, L. Mi, H. Wang, Z. Zhu, Q. Wu, Y. Zhang, Y. Jiang, *Small* **12**, 1062 (2016).
8. W. Choi, M. Y. Cho, A. Konar, J. H. Lee, G. B. Cha, S. C. Hong, S. Kim, J. Kim, D. Jena, J. Joo, S. Kim, *Adv. Mater.* **24**, 5832 (2012).
9. D. J. Late, P. A. Shaikh, R. Khare, R. V. Kashid, M. Chaudhary, M. A. More, S. B. Ogale, *ACS Appl. Mater. & Interf.* **6**, 15881 (2014).
10. M. Bernardi, M. Palummo, J. C. Grossman, *Nano Letters* **13**, 3664 (2013).
11. G. L. Frey, K. J. Reynolds, R. H. Friend, H. Cohen, Y. Feldman, *J. Amer. Chem. Soc.* **125**, 5998 (2003).
12. D. J. Late, Y. K. Huang, B. Liu, J. Acharya, S. N. Shirodkar, J. Luo, A. Yan, D. Charles, U. V. Waghmare, V. P. Dravid, C. N. R. Rao, *ACS Nano* **7**, 4879 (2013).
13. G. Eda, H. Yamaguchi, D. Voiry, T. Fujita, M. Chen, M. Chhowalla, *Nano Lett.***11**, 5111 (2011).
14. Y. Peng, Z. Meng, C. Zhong, J. Lu, W. Yu, Y. Jia, Y. Qian, *Chem. Lett.* **30**, 772 (2001).
15. R. Kaindl, B. C. Bayer, R. Resel, T. Müller, V. Skakalova, G. Habler, R. Abart, A. S. Cherevan, D. Eder, M. Blatter, F. Fischer, J. C. Meyer, D. K. Polyushkin, W. Waldhauser, *Beilstein J. Nanotechn.* **8**, 1115 (2017).
16. S. L. Wong, H. Liu, D. Chi, *Progr. Cryst. Growth Character. Mater.* **62**, 9 (2016).
17. V. Dhyani, P. Dwivedi, S. Dhanekar, S. Das, *Appl. Phys. Lett.* **111**, 191107 (2017).
18. A. Antonelou, G. Syrrokostas, L. Sygellou, G. Leftheriotis, V. Dracopoulos, S. N. Yannopoulos, *Nanotechn.* **27**, 045404 (2015).
19. X. Zhang, W. P. Han, J. B. Wu, S. Milana, Y. Lu, Q. Q. Li, A. C. Ferrari, P. H. Tan, *Phys. Rev. B* **87**, 115413 (2013).
20. H. N. T. Phung, V. N. K. Tran, L. T. Nguyen, L. K. T. Phan, P. A. Duong, H. V. T. Le, *J. Nanomater.* **2017** (2017).
21. A. Jäger-Waldau, M. C. Lux-Steiner, E. Bucher, L. Scandella, A. Schumacher, R. Prins, *Appl. Surf. Sci.* **65**, 465 (1993).